S100A1 Gene Therapy Preserves *in Vivo* Cardiac Function after Myocardial Infarction

Sven T. Pleger,[1,2,*] Andrew Remppis,[1,*] Beatrix Heidt,[1,*] Mirko Völkers,[1] J. Kurt Chuprun,[2] Matthew Kuhn,[2] Rui-Hai Zhou,[2] Erhe Gao,[2] Gabor Szabo,[3] Dieter Weichenhan,[1] Oliver J. Müller,[1] Andrea D. Eckhart,[2] Hugo A. Katus,[1] Walter J. Koch,[2,*,†] and Patrick Most[1,2,*,‡]

[1]*Medizinische Universitätsklinik und Poliklinik III, Otto Meyerhof Zentrum, Universität zu Heidelberg, INF 350, 69115 Heidelberg, Germany*
[2]*Center for Translational Medicine, Jefferson Medical College, 1025 Walnut Street, Philadelphia, PA 19107, USA*
[3]*Chirurgische Klinik der Universität Heidelberg, Abteilung für Herzchirurgie, INF 110, 69120 Heidelberg, Germany*

*These authors contributed equally to this work.

†*To whom correspondence and reprint requests should be addressed. Fax: +215 503 5728. E-mail: walter.koch@jefferson.edu.*

‡*To whom correspondence and reprint requests should be addressed. Fax: +49 6221 56 7632. E-mail: patrick_most@med.uni-heidelberg.de.*

Available online 15 September 2005

Myocardial infarction (MI) represents an enormous clinical challenge as loss of myocardium due to ischemic injury is associated with compromised left ventricular (LV) function often leading to acute cardiac decompensation or chronic heart failure. S100A1 was recently identified as a positive inotropic regulator of myocardial contractility *in vitro* and *in vivo.* Here, we explore the strategy of myocardial S100A1 gene therapy either at the time of, or 2 h after, MI to preserve global heart function. Rats underwent cryothermia-induced MI and *in vivo* intracoronary delivery of adenoviral transgenes (4×10^{10} pfu). Animals received saline (MI), the S100A1 adenovirus (MI/AdS100A1), a control adenovirus (MI/AdGFP), or a sham operation. S100A1 gene delivery preserved global *in vivo* LV function 1 week after MI. Preservation of LV function was due mainly to S100A1-mediated gain of contractility of the remaining, viable myocardium since contractile parameters and Ca^{2+} transients of isolated MI/AdS100A1 myocytes were significantly enhanced compared to myocytes isolated from both MI/AdGFP and sham groups. Moreover, S100A1 gene therapy preserved the cardiac β-adrenergic inotropic reserve, which was associated with the attenuation of GRK2 up-regulation. Also, S100A1 overexpression reduced cardiac hypertrophy 1 week post-MI. Overall, our data indicate that S100A1 gene therapy provides a potential novel treatment strategy to maintain contractile performance of the post-MI heart.

Key Words: gene therapy, myocardial infarction, contractile function, S100A1

INTRODUCTION

Cardiovascular disease accounts for nearly 40% of all deaths annually in Western countries. In particular, myocardial infarction (MI) represents an enormous clinical challenge as loss of myocardium is associated with compromised left ventricular (LV) function often leading to acute cardiac decompensation or chronic heart failure (HF) [1]. Recent advances in clinical therapy have reduced the overall mortality rate due to heart disease; however, therapies often fail to preserve global heart function during the post-MI period [2]. Therefore, novel therapeutic approaches to improve contractile properties of the remaining myo-cardium and thus prevent chronic HF are of great interest.

S100A1, a Ca^{2+}-binding protein of the EF-hand type, is preferentially expressed in the healthy heart and has recently been identified as a positive inotropic regulator of *in vivo* and *in vitro* myocardial contractility with cardioprotective actions at least *in vitro* [3–7]. Chronic cardiac inotropic effects observed in S100A1 transgenic mice were found to be independent of β-adrenergic signaling and were not accompanied by any detrimental effects on cardiac morphology or function chronically [5]. Importantly, S100A1 expression levels in myocardial tissue are significantly down-regulated in end-stage HF

[8,9]. Most recently, we could provide first evidence for the therapeutic impact of cardiac S100A1 gene delivery in the context of HF. Intracoronary delivery of the human S100A1 gene by the use of a first-generation adenovirus normalized diminished S100A1 protein abundance in an established chronic HF model of the rat that in turn rescued both impaired contractile performance and Ca^{2+} cycling of the failing myocardium *in vitro* and *in vivo* [9]. Mechanistically, S100A1-mediated effects on both healthy and failing cardiomyocytes are due to increased sarcoplasmic reticulum (SR) Ca^{2+}-ATPase (SERCA2a) activity, diminished diastolic SR Ca^{2+} leak, and augmented systolic open probability of the ryanodine receptor (RyR) causing an overall significant gain in both SR Ca^{2+} cycling and excitation–contraction coupling [4–6,9,10]. Further, S100A1 has recently been shown both to increase cardiac sarcomeric compliance and to modulate Ca^{2+} responsiveness of cardiac myofilaments that, in addition, might support the beneficial contractile effects seen in S100A1-overexpressing myocardium [4,11,12].

However, cardiac S100A1 gene transfer in an acute MI setting has not yet been examined and based on our previous studies, this might be advantageous as a mechanism to preserve global LV function. To support this hypothesis, data generated from S100A1 knockout mice demonstrate an inability of the heart to adapt to acute and chronic hemodynamic stress *in vivo* [13]. However, there are enormous differences between the transgenic mouse paradigm and exogenous gene transfer to adult animals and it is unknown whether the beneficial therapeutic S100A1 gene transfer approach in overt failing myocardium would also be effective in an acute clinical setting like MI. Over the past few years myocardial gene delivery has been shown to represent a powerful tool to alter myocardial function *in vivo* [9,14–17]. In this study, we sought to employ the apparent therapeutic properties of S100A1 following myocardial gene transfer, including a clinically relevant delivery protocol, to support remaining myocardium after acute MI and potentially to preserve global cardiac function and prevent chronic post-MI HF.

RESULTS

Acute Myocardial Infarction
Triphenyltetrazolium chloride (TTC) staining in LV sections at the midventricular level 6 h after cryoinfarction (Fig. 1A) or sham operation (Fig. 1B) shows representative infarct size. The use of the 8-mm cryostamp resulted in an average infarct size of 31.4 ± 2.2% of the LV (*n* = 8) as delineated by TTC staining. The cryothermia-mediated MI also resulted in a thinned LV free wall 7 days following MI (Fig. 1C) compared to sham-operated hearts (Fig. 1D).

Myocardial Gene Delivery and S100A1 Expression
Intracoronary delivery at the time of MI (0 h) of 4×10^{10} pfu of AdS100A1, AdGFP, or Adβ-gal resulted in robust infection of myocardium as assessed by X-gal staining (Figs. 2A and 2B), green fluorescent protein (GFP) fluorescence (Figs. 2C and 2D), or S100A1 immunohistochemistry (Figs. 2E and 2F) in LV cryosections. The distribution of marker genes was global in nature although not homogeneous (Figs. 2A–2D) as described previously [9,15]. This distribution pattern was also evident with S100A1 gene transfer as confirmed by immunohistochemistry using an antibody specific for the human isoform of S100A1 (Figs. 2E and 2F). Figs. 2G and 2H illustrate representative protein immunoblotting analysis carried out for S100A1 from LV homogenates showing specifically the human isoform in the AdS100A1-treated hearts. *In vivo* delivery of AdS100A1 resulted in readily detectable myocardial expression of the human isoform of S100A1 protein, whereas we were not able to detect human S100A1 protein in control groups (Fig. 2H). Quantification of total S100A1 mRNA expression levels in LV myocardium revealed a significant approximately fivefold overexpression in AdS100A1-treated animals compared to all control groups (Fig. 2I).

Figs. 2J–2L show the representative proportion of GFP-stained myocytes 2 h after cell isolation and Ca^{2+} toleration. Within 26 randomly chosen field of views 132 of 743 isolated myocytes exhibited GFP staining (17.7%) 7 days after *in vivo* gene delivery and MI. We confirmed overexpression of total S100A1 mRNA in isolated cardiomyocytes used for cell contractility studies (Fig. 2N). Expression of the endogenous S100A1 isoform was unchanged 1 week after gene transfer compared to control groups using rat S100A1 primers, which lack detection of the human isoform (Fig. 2O).

Preservation of *in Vivo* Myocardial Function after Acute MI through S100A1 Gene Therapy
We determined the *in vivo* functional consequences of myocardial S100A1 gene therapy at 0 h in this acute MI model 1 week after MI using a closed-chest cardiac catheterization technique. We recorded LV pressure in anesthetized animals under basal conditions and in response to acute hemodynamic stress provoked by continuous epinephrine infusion. Figs. 3A–3D depict baseline hemodynamic parameters of infarcted and AdS100A1-treated rats (MI/AdS100A1, *n* = 8) compared to infarcted rats treated with saline (MI, *n* = 6) or AdGFP (MI/AdGFP, *n* = 6) and noninfarcted controls (sham, *n* = 7) 7 days following MI and *in vivo* gene delivery. Cryothermia-induced acute loss of LV myocardium resulted in significantly reduced cardiac contractility as assessed by the maximal rate of LV pressure rise (+*dP/dt*) and fall (−*dP/dt*) 7 days following MI (Figs. 3A and 3B). Moreover LV end systolic pressure (ESP) was significantly reduced, while end diastolic pressure (EDP) was
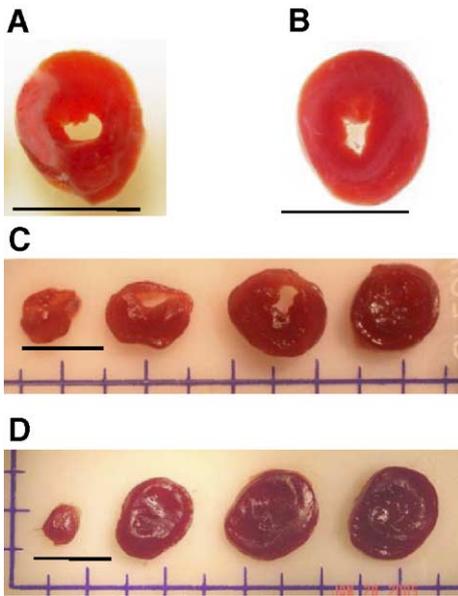
FIG. 1. Model of cryomyocardial infarction (MI). Representative TTC-stained cross sections at the midventricular level 6 h after (A) MI or (B) sham operation. Scale bar, 10 mm. (C) Representative cross sections of the heart demonstrating the effect of MI on LV geometry 7 days after MI compared to (D) sham. Scale bar, 10 mm.

heart rate (HR) was unaltered 7 days after MI (data not shown).

S100A1 gene delivery at the time of MI resulted in significant improvements in hemodynamic parameters 7 days later compared to AdGFP- and saline-treated MI rats. Myocardial S100A1 protein overexpression significantly increased the $+dP/dt$ by 30.8% and the $-dP/dt$ by 24.5% compared to MI/AdGFP under basal conditions *in vivo* (Figs. 3A and 3B). In addition, S100A1 overexpression resulted in significantly enhanced LV end systolic pressure compared to control animals (Fig. 3C). LV EDP tended to be decreased in AdS100A1-treated rats although this observation was not statistically significant. Of importance, S100A1 gene transfer did not affect HR (data not shown) 7 days after MI. Interestingly, overexpression of human S100A1 in the infarcted rat heart caused a therapeutic gain in baseline cardiac hemodynamic function that actually could not be statistically distinguished from healthy, sham-operated animals (Figs. 3A–3D).

When we challenged infarcted and AdS100A1-treated rats in this delivery protocol (0 h) with epinephrine, *in vivo* LV performance was significantly enhanced compared to MI/AdGFP and MI controls. Thus, in addition to increased cardiac contractility observed under basal conditions, AdS100A1-treated rats had a larger cardiac reserve to respond to acute hemodynamic stress seen with $+dP/dt$, $-dP/dt$, and LV end systolic pressure (Figs. 3E–3G). In addition, under β-adrenergic stimulation, EDP

significantly increased (Figs. 3C and 3D). Additionally, the time constant of monoexponential isovolumetric pressure decay (τ) was significantly extended, while
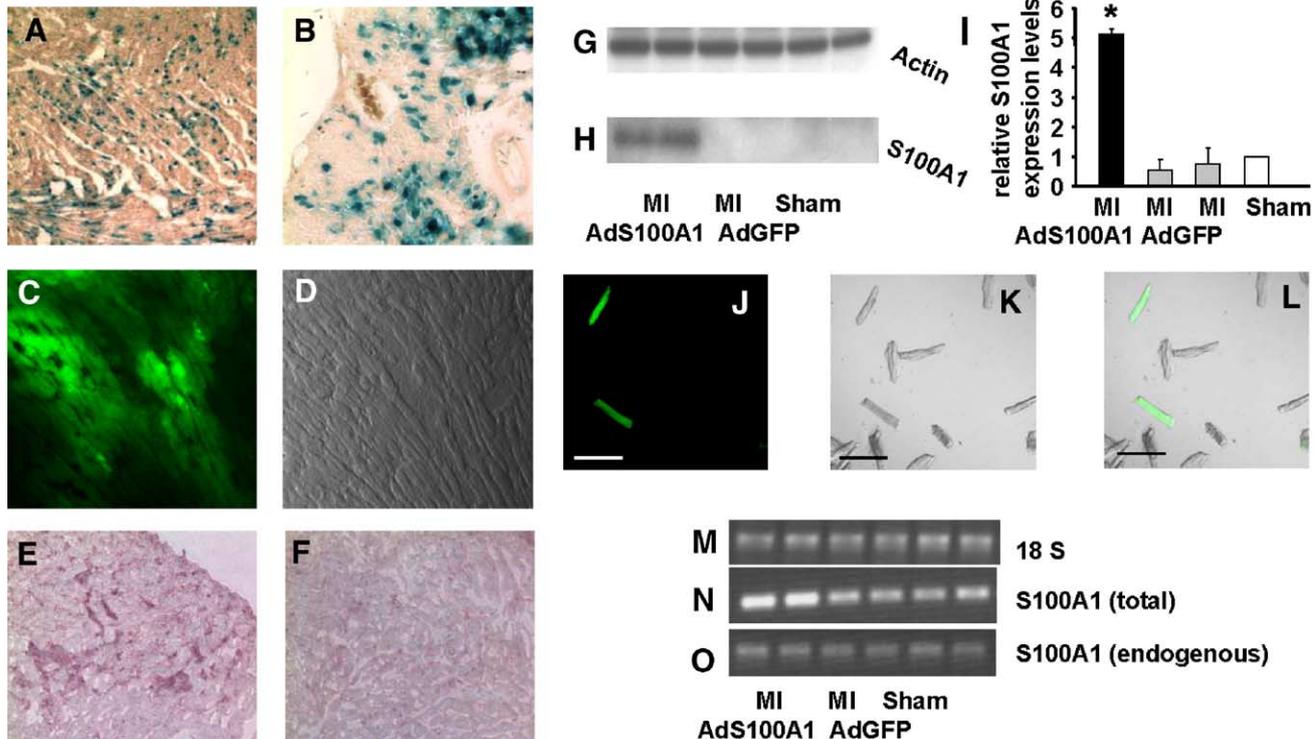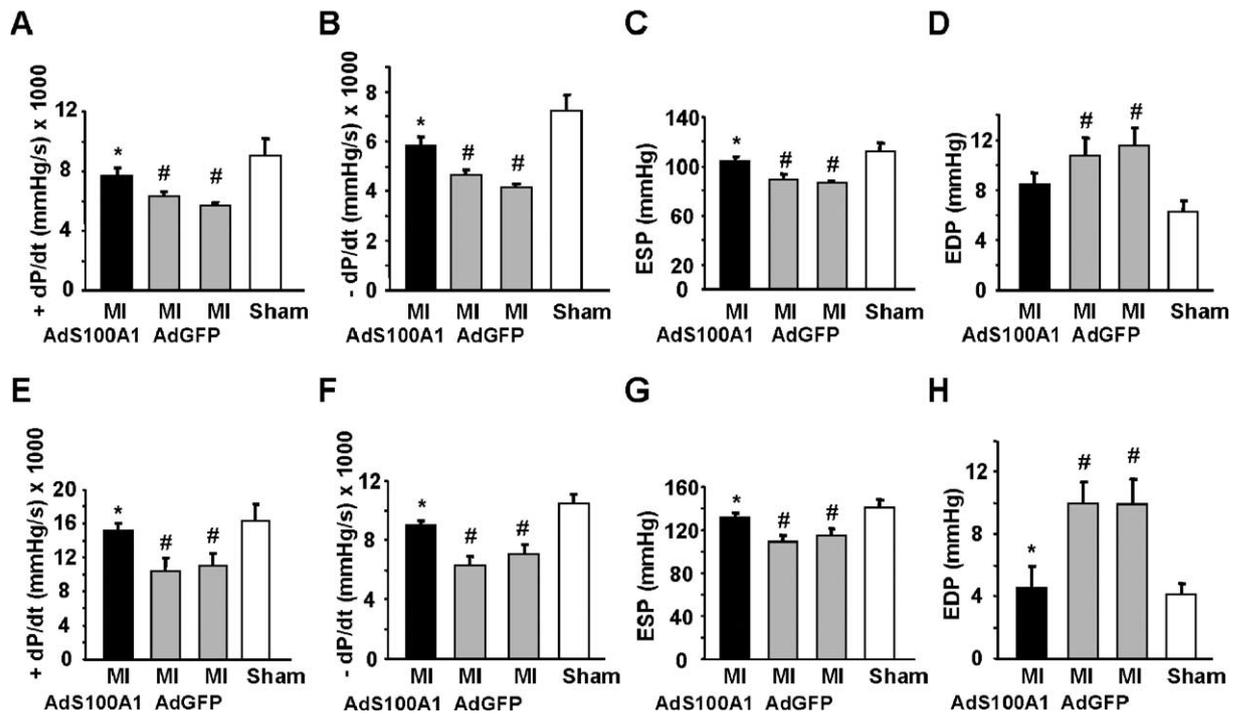
FIG. 3. Assessment of *in vivo* cardiac contractile function. (A–D) Myocardial S100A1 *in vivo* gene delivery preserves basal cardiac function compared to sham and significantly increases contractile parameters compared to MI and MI/AdGFP. (E–H) AdS100A1 treatment preserves cardiac function of post-MI hearts under acute hemodynamic stress using a maximal dose of epinephrine (5 μg/kg BW/min). Data were obtained 7 days after MI and gene transfer. Sham $n = 7$, MI/AdS100A1 $n = 8$, MI $n = 6$, MI/AdGFP $n = 6$. #$P < 0.05$ compared to sham. *$P < 0.05$ compared to MI/AdGFP and MI groups. ANOVA and Bonferroni test between all groups. Data are presented as means ± SEM.

was significantly reduced in MI/AdS100A1 animals compared to MI/AdGFP and MI controls (Fig. 3H). As under basal conditions, HR was not statistically different after β-adrenergic stimulation (data not shown). Moreover, cardiac contractility of AdS100A1-treated infarcted rats did not differ significantly from that of noninfarcted sham-operated rats 7 days after MI (Figs. 3E–3H).

S100A1 Gene Therapy Increases Contractile Properties and Ca²⁺ Transients of Cardiomyocytes post-MI

To determine whether changes in cellular Ca^{2+} cycling account for the preserved cardiac contractility of AdS100A1-treated rats in the acute post-MI period, we examined contractile performance and intracellular Ca^{2+} handling in ventricular myocytes isolated from rats in the

different experimental groups (0 h gene delivery). Interestingly, in single isolated myocytes, the amplitude of the $[Ca^{2+}]_i$ transients, the fractional shortening (FS), the rate of myocyte shortening ($-dL/dt$), and the rate of myocyte relengthening ($+dL/dt$) remained unchanged between myocytes isolated from MI/AdGFP ($n = 40$), MI ($n = 33$), and sham-operated ($n = 30$) animals 7 days post-MI (Figs. 4A–4D). Therefore, even though global hemodynamics showed dysfunction, at the myocyte level contractile function was still relatively normal 7 days post-MI.

Despite no detrimental function at the myocyte level 7 days post-MI, S100A1-overexpressing myocytes from MI/AdS100A1 rats ($n = 27$) showed significantly enhanced $[Ca^{2+}]_i$ transients and contractile properties as assessed by $-dL/dt$, $+dL/dt$, and FS compared to myocytes derived

FIG. 2. Intracoronary S100A1 *in vivo* gene delivery. (A and B) Representative β-galactosidase expression and (C) GFP fluorescence microscopy and (D) corresponding light microscopy of LV myocardium 7 days after MI and *in vivo* gene transfer. Original magnification, 10× (A), 20× (B), 40× (C, D). (E and F) S100A1 immunohistochemistry. Frozen LV tissue sections from (E) AdS100A1-treated and (F) AdGFP-treated rats were prepared and analyzed for human S100A1 by immunohistochemistry as described under Materials and Methods. Positive staining is in purple. Original magnification, 20×. (G and H) Representative Western blot analysis of actin and human S100A1 in LV homogenates of sham, MI/AdGFP, and MI/AdS100A1 rats 7 days after *in vivo* gene delivery. (I) Quantification of total LV S100A1 mRNA expression levels by RT-PCR 7 days after *in vivo* gene delivery; *$P < 0.05$ compared to MI/AdGFP, MI, or sham (three experiments; MI/AdS100A1 $n = 8$, MI/AdGFP $n = 8$, MI $n = 7$; sham $n = 8$). Two hours after myocyte isolation GFP expression was used to identify *in vivo* treated cells. (J) GFP fluorescence. (K) Light microscopy. (L) Overlay of J and K. Scale bar, 100 μm. (M–O) mRNA expression of isolated LV cardiomyocytes. (M) 18S rRNA; (N) total S100A1, $P < 0.05$ MI/AdS100A1 vs MI/AdGFP or sham (three experiments, $n = 3$ for each group); and (O) endogenous S100A1, $P = NS$ between all groups (three individual experiments, $n = 3$ for each group). ANOVA and Bonferroni test between all groups.
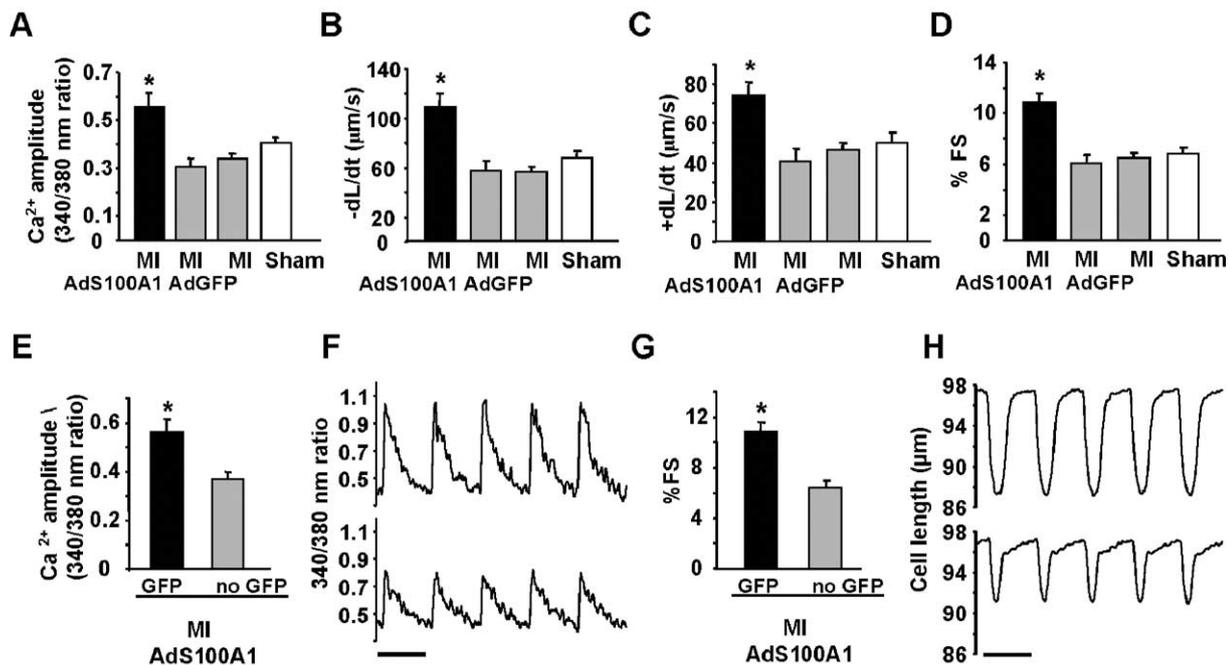
FIG. 4. Intracoronary S100A1 gene delivery increases contractility and intracellular Ca^{2+} transients of isolated cardiomyocytes. Cells were isolated 7 days after MI and *in vivo* gene delivery. Cells were measured 2 h following myocyte isolation. (A) Ca^{2+} amplitude (340/380 nm ratio), (B) rate of cell shortening ($-dL/dt$; μm/s), (C) rate of cell relengthening ($+dL/dt$; μm/s), and (D) percentage of cell shortening (%FS). Sham $n = 30$, MI $n = 33$, MI/AdS100A1 $n = 27$, MI/AdGFP $n = 40$. Cells were isolated from three different rats per group. *$P < 0.05$ compared to MI/AdGFP, MI, or sham. ANOVA and Bonferroni test between all groups. Data are presented as means $\pm$ SEM. (E–H) Increased contractile function of S100A1-infected cardiomyocytes (GFP) compared to uninfected cells (no GFP) isolated from the same AdS100A1-treated rat post-MI. GFP fluorescence was used to differentiate between *in vivo* infected and *in vivo* uninfected cardiomyocytes. (E) Ca^{2+} amplitude (340/380 nm ratio), (F) representative raw traces of Ca^{2+} transients of S100A1-treated (top) and untreated cardiomyocytes (bottom), (G) percentage of cell shortening, (H) representative tracings of cell length of S100A1-treated (top) and untreated cardiomyocytes (bottom). MI/AdS100A1–GFP $n = 27$, MI/AdS100A1–no GFP $n = 20$. Cells were isolated from three different rats per group. *$P < 0.05$ compared to MI/AdS100A1–no GFP. Student's *t* test. Data are presented as means $\pm$ SEM. Bar, 1 s.

from MI/AdGFP, MI, and sham-operated animals (Figs. 4A–4D). Diastolic cell length did not differ significantly in all groups (data not shown). We could select myocytes infected with AdS100A1 due to this vector also having a GFP transgene. Contractility and Ca^{2+} transients in ventricular myocytes from AdS100A1-treated rats 7 days post-MI were significantly increased even in comparison to myocytes derived from noninfarcted sham rats. Moreover, $[Ca^{2+}]_i$ transients and contractile parameters of S100A1-overexpressing myocytes were also significantly augmented compared to uninfected cells ($n = 28$) isolated from the same MI/AdS100A1 animals (Figs. 4E–4H). Taken together, these results demonstrate that the preserved global *in vivo* cardiac function of S100A1-treated animals post-MI might be attributed to enhanced contractile properties and $[Ca^{2+}]_i$ transients of remaining myocardium (noninfarcted) overexpressing S100A1.

S100A1 Gene Therapy 2 h after Acute MI
To investigate any clinical potential of a S100A1 gene therapy approach in the acute MI setting, we delivered AdS100A1 ($n = 8$) 2 h after MI. Importantly, treatment under these more clinical delivery conditions (some time

after the infarct) also resulted in significantly increased cardiac contractile parameters 7 days after MI compared to both MI ($n = 8$) and MI/AdGFP ($n = 7$) as revealed by echocardiography and cardiac catheterization (Table 1). These physiological results are nearly identical to what we found when the viruses were delivered at the time of MI (0 h). Cardiac function of infarcted AdS100A1-treated rats was not significantly different from that of sham ($n = 8$) although MI/S100A1 rat hearts trended toward slightly reduced contractile parameters from sham animals (Table 1). In contrast, MI and MI/GFP groups showed a significantly depressed heart function compared to both sham and MI/S100A1 (Table 1). Importantly, while β-adrenergic responsiveness was significantly ablated in MI and MI/AdGFP groups, S100A1 gene therapy nearly preserved the cardiac inotropic reserve in response to a maximal dose of isoproterenol compared to sham (Table 1; Figs. 5A and 5B).

Investigation of Representative Markers of Heart Failure and Myocardial Hypertrophy
Since MI often causes progressive deterioration of cardiac function and transition to HF, we investigated

TABLE 1: Clinical relevance of S100A1 gene therapy					
	Sham operation (*n* = 8)	MI–saline (*n* = 8)	MI/AdGFP (*n* = 7)	MI/AdS100A1 (*n* = 8)	*P*
Basal LV catheterization					
HR (min^{-1})	339 ± 5.4	328 ± 10.6	320 ± 9.5	330 ± 11.7	NS
LV +*dP/dt* (mm Hg/s)	6,974 ± 289	6,064 ± 221	5695 ± 171	7,453 ± 383	**,***
LV −*dP/dt* (mm Hg/s)	7,174 ± 310	5,452 ± 249	5198 ± 115	6,470 ± 341	**,***
LVESP	123 ± 2.7	107 ± 3.7	102 ± 2.3	114 ± 4.2	**,***
LVEDP	1.3 ± 0.9	4.4 ± 0.9	5.2 ± 0.3	1.7 ± 0.3	***
Echo					
LVIDs (mm)	3.54 ± 0.09	5.75 ± 0.15	5.8 ± 0.13	4.11 ± 0.21	**,***
LVIDd (mm)	6.23 ± 0.15	7.33 ± 0.12	7.4 ± 0.15	6.58 ± 0.19	**,***
FS (%)	43.6 ± 0.28	24.4 ± 1.2	21.2 ± 0.85	38.3 ± 2.3	**,***
EF (%)	73.7 ± 0.28	46.8 ± 1.9	41.8 ± 1.4	66.5 ± 2.9	**,***
PWTd (mm)	1.25 ± 0.08	1.23 ± 0.05	1.26 ± 0.04	1.28 ± 0.05	NS
Isoproterenol (333 ng/kg BW)					
HR (min^{-1})	414 ± 6.8	399 ± 12.6	389 ± 12.7	396 ± 7.0	NS
LV +*dP/dt* (mm Hg/s)	15,213 ± 356	10,442 ± 421	9723 ± 289	14,141 ± 342	**,***
LV −*dP/dt* (mm Hg/s)	8,685 ± 275	5,826 ± 325	5285 ± 338	7,238 ± 369	*,**,***
LVESP	124 ± 3.6	109 ± 2.4	106 ± 3.8	126 ± 2.3	**,***
LVEDP	2.0 ± 3.6	5.3 ± 0.5	3.6 ± 0.2	1.2 ± 0.5	**,***
Δ +*dP/dt* (mm Hg/s)	8,239 ± 317	4,378 ± 318	4028 ± 236	6,688 ± 321	*,**,***

Treatment with saline, AdGFP, or AdS100A1 was performed 2 h after MI. Data were obtained from rats 7 days after MI. LV +*dP/dt,* first derivative of LV pressure rise, LV −*dP/dt* first derivative of LV pressure fall; HR, heart rate; LVESP, LV end systolic pressure; LVEDP, LV end diastolic pressure; Δ +*dP/dt,* increase in LV +*dP/dt* under maximal β-adrenergic stimulation; LVIDd, LV inner diameter during diastole; LVIDs, LV inner diameter during systole; FS, fractional shortening; EF, ejection fraction; PWTd, posterior wall thickness in diastole; NS, nonsignificant. ANOVA and Bonferroni test between all groups. Data are presented as means ± SEM.

   *   *P* < 0.05 MI/AdS100A1 compared to sham.
  ** *P* < 0.05 MI/AdS100A1 compared to MI and MI/AdGFP groups.
*** *P* < 0.05 sham compared to MI and MI/AdGFP.

the expression pattern of marker proteins reflecting this process. We determined the expression levels of the Ca^{2+}-cycling proteins SERCA2a, PLB, and NCX in rat hearts treated with viruses 2 h after MI. These proteins are known to be altered in the transition to HF and S100A1 can alter Ca^{2+} cycling in the myocyte. We also examined the expression of the G-protein-coupled receptor kinase 2 (GRK2 or βARK1) since this kinase is up-regulated in HF and its increased expression has been shown to decrease β-adrenergic inotropic reserve in dysfunctional hearts [18]. While SERCA2a, PLB, and NCX mRNA expression was not altered by either MI or S100A1 gene delivery (data not shown), GRK2 expression was significantly up-regulated in MI and MI/GFP hearts but not in MI/S100A1 rat hearts 7 days after MI (Fig. 5C). We examined ANF mRNA expression levels as a marker of myocardial hypertrophy [19,20] and ANF was significantly increased in infarcted rats compared to the sham group 7 days post-MI (Fig. 5D). In AdS100A1-treated MI rats ANF expression was significantly lower compared to both MI and MI/AdGFP groups (Fig. 5D). Consistent with ANF expression results, heart weight to body weight ratio (HW/BW) was significantly increased in MI and MI/AdGFP groups compared to noninfarcted controls, while the HW/BW of MI rats treated with AdS100A1 was significantly lower and not different from that of sham control rats (Fig. 5E). Lung and liver weights were found to be unaltered between all groups investigated (data not shown).

DISCUSSION

S100A1 has been characterized as a novel positive inotropic factor and regulator of myocardial contractility *in vitro* and *in vivo* [4,21,22]. Effects mediated by intracellular S100A1 protein appear primarily based on improved SR Ca^{2+} cycling and altered sarcomeric function [4–7,9,12], while activity of sarcolemmal Ca^{2+} cycling proteins such as the L-type Ca^{2+} channel and the NCX are not affected by the protein [10]. In fact, enhanced SERCA2a activity as well as improved RyR function appears to be the major mechanism for S100A1-mediated rescue of a chronic HF model in the rat [9]. Given these results and findings in S100A1-knockout mice showing an inability of these hearts to adapt to acute and chronic hemodynamic stress *in vivo* [13], we wanted to investigate in this study whether S100A1 gene delivery around the time of MI could prevent more acute LV dysfunction. Our findings show quite clearly that the S100A1 protein can mediate improved cardiac function following acute MI. Importantly, this was seen in an experimental group in which AdS100A1 was delivered via our intracoronary gene delivery techniques 2 h after MI, demonstrating a potentially clinically relevant molecular
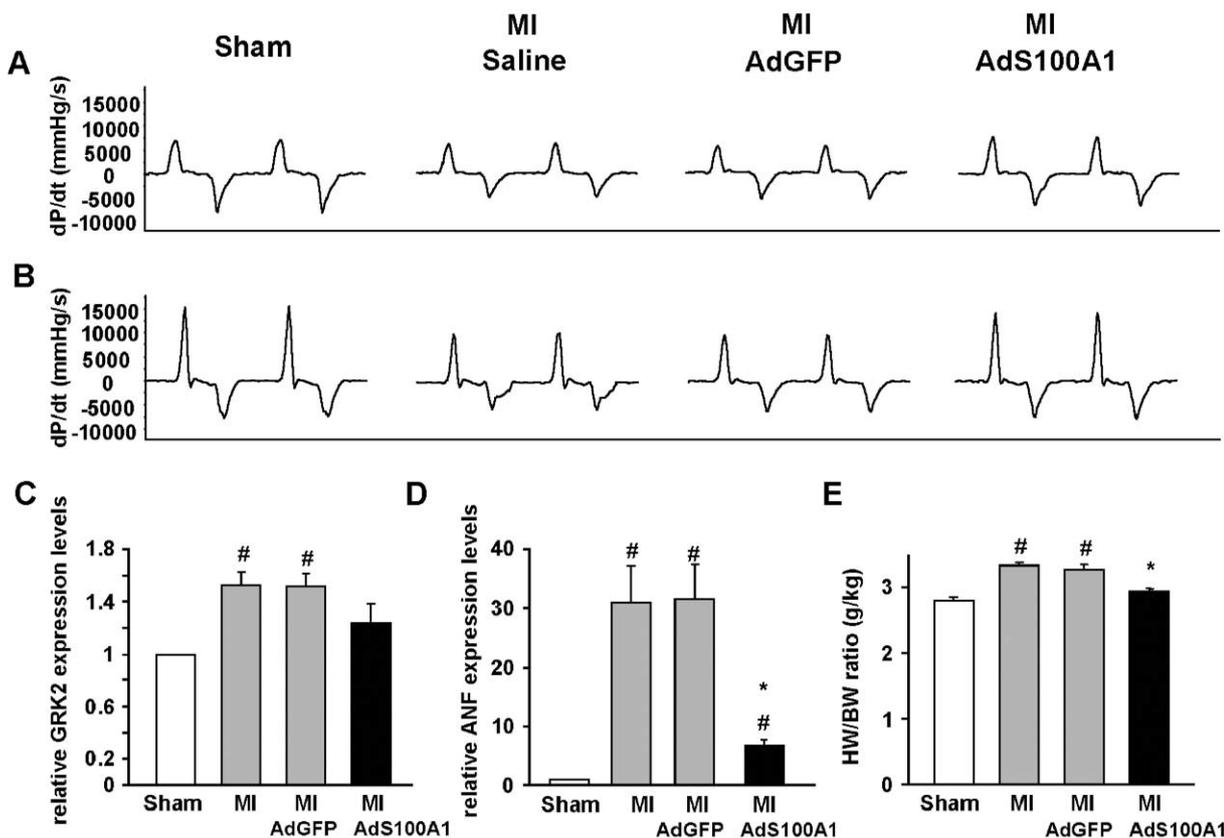
FIG. 5. Preservation of cardiac inotropic reserve after MI due to S100A1 gene therapy. Original tracings of *dP/dt* of sham, MI, MI/AdGFP, and MI/AdS100A1 groups (A) under basal conditions and (B) under maximal β-adrenergic stimulation. (C) Decreased cardiac inotropic reserve 7 days after MI was associated with significantly increased expression levels of GRK2. S100A1 gene therapy attenuated the increase in GRK2 expression after MI. (D and E) Analysis of hypertrophy. (D) Ventricular ANF mRNA levels of MI/AdS100A1, MI/GFP, and MI relative to sham and standardized to 18S rRNA in LV myocardium and (E) HW/BW ratio 7 days after MI and gene delivery. MI/AdS100A1 $n = 8$, MI/AdGFP $n = 8$, MI $n = 7$, sham $n = 8$. #$P < 0.05$ compared to sham. *$P < 0.05$ compared to MI and MI/AdGFP. ANOVA and Bonferroni test between all groups. Data are presented as means ± SEM.

therapeutic strategy in which the S100A1 protein can have a beneficial effect in the acute MI setting.

In the MI model employed, *in vivo* cardiac function is severely depressed within a week after the injury. When S100A1 is overexpressed following acute post-MI gene delivery, this 7-day post-MI dysfunction is prevented and virtually normal *in vivo* cardiac function is preserved. This functional normalization occurs even in the face of a significant proportion of the LV infarcted. Thus, S100A1 overexpression increases the contractility of remaining viable myocardium, which is responsible for our observed *in vivo* findings. Functional benefit was seen both basally and after β-adrenergic stimulation *in vivo*, indicating a preserved inotropic reserve after S100A1 gene delivery and protein overexpression. This increased inotropic reserve is consistent with previous results in S100A1 transgenic mice [5]. Interestingly, a mechanism for this in the current study was found as S100A1-treated post-MI hearts lacked significant GRK2 up-regulation that was a characteristic of the post-MI

(and MI-AdGFP-treated) hearts. Enhanced GRK2 expression has been implicated in the maladaptive desensitization of β-adrenergic receptors (β-ARs) in the dysfunctional LV [18]. Therefore, S100A1-mediated preservation of global *in vivo* cardiac function might diminish dysfunctional cardiac β-AR signaling that is part of the transition to HF.

We also found that 7 days after MI there was significantly elevated HW/BW and up-regulation of ventricular ANF expression, indicating that post-MI hearts were hypertrophic. S100A1 overexpression prevented post-MI hypertrophy as ANF levels were significantly decreased and hearts were of normal size. Thus, preservation of global function by S100A1 gene transfer appears to be able to prevent hypertrophic changes associated with MI that can often lead to LV remodeling and HF. It should be noted that although hypertrophy was present 7 days post-MI, altered expression of other markers of HF was not evident as SERCA2a, PLB, and NCX levels were similar in all groups.

Interestingly, although globally the contractility of post-MI hearts was significantly depressed, myocytes isolated 7 days post-MI exhibited unchanged intracellular Ca^{2+} transients and contractile parameters compared to myocytes obtained from sham-operated animals. Therefore, the impairment of global cardiac function *in vivo* appears to involve primarily the loss of viable myocardium and the lack of contractile mass, while at the cellular level, no significant transition to dysfunction or failure is present. It is noteworthy that impaired LV contractility without cellular contractile dysfunction in the early postinfarct period is in line with several studies and the sudden loss of myocardium was shown to play the most important role in initiating global LV dysfunction after acute MI [23,24]. It is important to note that contractility at the cellular level was measured under unloaded conditions, while the MI-mediated decrease of global cardiac function was seen *in vivo*.

Contractile parameters and $[Ca^{2+}]_i$ transients of AdS100A1-treated myocytes derived from infarcted hearts were significantly increased compared to both MI/AdGFP- and sham-derived myocytes. These findings provide evidence that the therapeutic effect of S100A1 *in vivo* gene therapy in acute MI is most probably due to an enhancement of the remaining myocardium by AdS100A1-infected myocytes compensating for lost myocardium. Moreover, uninfected myocytes might be indirectly supported by the integration into the invigorated remaining myocardium.

In the clinical situation, we argue that myocardial gene therapy using S100A1 to preserve global cardiac contractility in the acute post-MI period could be beneficial, and chronically this could prevent cardiac remodeling and progressive deterioration of LV function that can occur [25]. Unfortunately in the present study, we could not address these chronic issues and determine if S100A1 can permanently prevent the transition to HF since we used a first-generation adenoviral vector and our S100A1 overexpression was absent after 21 days (data not shown). In fact, cardiac function measured 3 weeks after MI showed that AdS100A1-treated MI hearts were now dysfunctional since S100A1 was not increased (data not shown). Thus, longer studies will have to be done in the future with advanced vectors allowing for a longer duration of expression, such as adeno-associated viral vectors [26]. Importantly, the size of the cryothermia-induced myocardial damage was shown to be located close to the area injured by the cryostamp without transition zones to viable myocardium [27], and the initial loss of contractile myocardium was highly reproducible. Since S100A1 overexpression was not present when MI occurred, S100A1 gene transfer had no effect on initial infarct size. Moreover, 21 days post-MI, after a period of significant S100A1 overexpression, infarct sizes in the LV did not differ significantly between MI/AdGFP and MI/AdS100A1

groups (data not shown), indicating that transient S100A1 overexpression did not influence the scar in this model.

In the post-MI period there also exist other approaches to preserve global cardiac contractility such as the replacement of lost cardiomyocytes using tissue replacement therapy or stem cell therapy approaches [28,29]. In this study, we demonstrate the feasibility of S100A1 gene therapy to support the remaining myocardium after MI and thus delay the development of significant LV dysfunction and subsequent HF. Recent advances in clinical therapy of MI have significantly reduced the acute mortality; however, often these measure fail to preserve cardiac function and prevent the transition to HF [1,2]. Therefore, S100A1 gene therapy may add to the established clinical concept of the treatment of MI. This approach appears to be supported by the finding that normalization of myocardial S100A1 expression levels has been shown to rescue end-stage HF [9].

Observations from Tsoporis *et al.* and our group suggest that S100A1 is involved in the maintenance of the genetic program that defines normal myocardial function and that its down-regulation is permissive for the induction of genes that underlie myocardial hypertrophy [9,30]. This feature is in line with the reduced hypertrophy and ANF expression in this study and might become even more beneficial in a chronic therapeutic S100A1 gene delivery approach. Chronic S100A1 overexpression might be advantageous to other positive inotropic proteins, since in S100A1 transgenic mice no detrimental effects were observed, while overexpression of the β_1-AR induces fibrosis, severe LV dysfunction, and arrhythmias [5,31].

To summarize, this study reports three novel findings. First, our results demonstrate for the first time that *in vivo* S100A1 gene therapy acutely after MI preserves global cardiac function, preventing LV dysfunction, which potentially may delay subsequent HF development. Moreover, these novel results could be achieved by using a clinically relevant time of treatment during the post-MI period. Second, preservation of systolic function is due to the S100A1-mediated gain of contractility of the remaining viable myocardium. Finally, we show that the S100A1 treatment maintains the cardiac β-adrenergic inotropic reserve after MI, which appears to be at least partially linked to the prevention of GRK2 up-regulation that is associated with cardiac injury and dysfunction. Therefore, S100A1 gene therapy might provide a novel treatment strategy for improving the cardiac performance of the post-MI heart.

MATERIALS AND METHODS

This investigation conformed to the *Guide for the Care and Use of Laboratory Animals* published by the U.S. National Institutes of Health (NIH Publication No. 85-23, revised 1996) and all procedures were approved by the appropriate institution committees.

Adenoviral vectors. First-generation early gene 1/3-deleted S100A1 adenovirus (AdS100A1) was obtained by the use of the pAdTrack-CMV/pAdEasy-1 system as previously described [4,32]. Expression of human S100A1 cDNA and GFP reporter gene was driven by a cytomegalovirus (CMV) promoter. The same adenovirus devoid of S100A1 cDNA served as control (AdGFP). Adβ-gal was used as described previously [17]. Replication-deficient adenoviruses were amplified in human embryonic kidney 293 cells, purified, and enriched by cesium chloride centrifugation as described [4]. The titer of stocks used for myocardial gene transfer was 2.1×10^{11} pfu/ml for AdGFP (bioactivity 29.5), 2.6×10^{11} pfu/ml (bioactivity 29.2) for AdS100A1, and 2.3×10^{11} pfu/ml (bioactivity 27.2) for Adβ-gal.

Myocardial infarction and adenoviral-mediated gene transfer. Anesthesia of adult male (250–300g) rats was induced using 5% isoflurane (v/v) mixed with oxygen. Anesthetized rats were intubated and mechanically ventilated (Hugo Sachs, Germany) and anesthesia was maintained using 2% isoflurane (v/v) mixed with oxygen. The heart was exposed through a median sternotomy and a 6-O suture was placed at the apex of the LV. To induce myocardial infarction an 8-mm-diameter cylindrical stamp was cooled in liquid nitrogen and then pressed on the LV free wall. Cryothermia was applied by use of three freeze cycles of 1 min each that was interrupted by 1-min thawing intervals [33].

Myocardial gene transfer was achieved as previously described [9,15]. Briefly, a 22-gauge catheter containing 200 μl of adenovirus was advanced from the apex of the LV to the aortic root and then 0.75 mg of adenosine was injected into the RV. The aorta and pulmonary arteries were clamped distal to the site of the catheter and the solution was rapidly injected, while the perfusion of the coronaries could be observed by a change of color of the heart. After 20 s the clamp on the aorta and pulmonary artery was released. The chest was then closed and animals were transferred back to their cages, receiving appropriate analgesia. In a second group of animals, the AdS100A1 was delivered 2 h after MI at a clinically relevant time of treatment. In those rats, the aorta was looped and the chest was closed after the cryoinfarction while anesthesia was maintained. Two hours after MI a catheter was advanced into the aortic root via the carotid artery to accomplish the myocardial gene delivery.

Catheter-based in vivo hemodynamic measurements. Seven days after gene delivery and MI, cardiac function was studied in each rat. Rats were sedated with ketamine (100 mg/kg) and xylazine (3 mg/kg) and a 2.5-F pressure-transducer (SPR-870; Millar Instruments, Houston, TX, USA) was placed into the LV cavity through the right carotid artery to record pressure and heart rate as previously described [9]. The right external jugular vein was cannulated with a 22-gauge catheter that was used for epinephrine infusion and saline injections. Data were obtained as steady-state cycles at baseline and after infusions of epinephrine (5.0 μg/kg/min). Rats treated 2 h after MI were anesthetized with isoflurane (2% v/v) and received increasing dosages of isoproterenol injections (3.3, 33.3, and 333 ng/kg BW).

Echocardiography. Echocardiography was performed with the Visual-SONICS VeVo 770 imaging system using a 710 scanhead in anesthetized animals (2% isoflurane (v/v) as previously described [34]. The internal diameter of the left ventricle was measured in the short-axis view from M-mode recordings in end diastole and end systole. VisualSONICS analysis software was used to calculate ejection fraction (EF) and FS using the formulas (LVIDd − LVIDs)/LVIDd × 100 (for LV %FS), $(\text{LV}(V_d) - \text{LV}(V_s))/\text{LV}(V_d) \times 100$ (for LV %EF), $(7/(2.4 + \text{LVIDd})) \times (\text{LVIDd})^3 \times 1000$ (for diastolic LV volume), and $(7/(2.4 + \text{LVIDs})) \times (\text{LVIDs})^3 \times 1000$ (for LV systolic volume). $\text{LV}(V_d)$ is LV diastolic volume and $\text{LV}(V_s)$ is LV systolic volume.

Infarct size. To examine the reproducibility of the infarct model, eight rats were euthanized 6 h after MI. Hearts were sectioned from apex to base into 2-mm slices. To delineate the infarct size, sections were incubated in 1% (wt/vol) TTC (Sigma) in PBS (pH 7.4) at 37°C for 15 min. For each section, the infarct size was measured from enlarged digital photos. Percentage MI was calculated as the infarcted area divided by the area of the whole LV of the section.

Isolation of adult ventricular rat cardiomyocytes. Ca^{2+}-tolerant adult cardiomyocytes were isolated from LV tissue of infarcted and gene-delivered or sham-operated rats by a standard enzymatic digestion procedure and cultivated as described [4,9]. Cardiomyocytes used for simultaneous contractility and Ca^{2+} measurements were plated at a density of 20,000 cells/cm² on laminin-coated glass dishes (Willco Wells; ⌀ 1 cm). For analysis of mRNA expression cardiomyocytes were plated on laminin-coated plastic dishes (Nunc; ⌀ 3.5 cm) at a density of 150,000 cells/cm².

Ca^{2+}-transient analyses and contractile parameters of isolated adult rat cardiomyocytes. Contractility and intracellular Ca^{2+} transients of Fura 2-AM-loaded (0.5 μmol/L for 20 min at 37°C) adult rat cardiomyocytes were measured simultaneously 2 h following myocyte isolation using the IonOptix MyoCam system (IonOptix Corp.) [9]. Myocytes were electrically stimulated with a biphasic pulse to contract at 37°C. Measurements were carried out using an inverse Olympus microscope (IX 71) with a dual-excitation single-emission fluorescence photomultiplier system and a video edge detection system (IonOptix Corp.). Twenty consecutive steady-state twitches for each myocyte at 1 Hz and 2 mM $[Ca^{2+}]_e$ were averaged and analyzed. Myocytes were isolated from three rats of each group (MI/AdS100A1, MI/AdGFP, MI, and sham). At least 10 myocytes per animal were measured. Within the MI/AdS100A1 and MI/AdGFP groups GFP staining was used to differentiate between infected (GFP) and uninfected myocytes (no GFP) isolated from the same animal.

In vivo gene therapy efficiency. Efficiency of *in vivo* gene transfer was assessed in cryosectioned hearts (20 μm) by expression of β-galactosidase as described previously [17] and by GFP fluorescence (510 nm) using an Olympus IX81 confocal microscope. To confirm specificity of the GFP emission, the same offset for suppressed background of untreated hearts excited at 488 nm was applied to both AdS100A1- and AdGFP-treated hearts and additional measurements were taken below and above the GFP excitation spectrum as described previously (data not shown) [9]. Additionally, percentage of GFP-stained isolated myocytes was assessed 7 days following *in vivo* gene transfer within 26 randomly assigned visual fields using an Olympus IX 71 microscope, a mercury arc light, and suitable filters.

Western blot analysis. Western blots were performed as described previously [4] to assess protein levels of S100A1 and cardiac α-actin. Whole rat LVs were homogenized at 4°C in PBS (wt/3vol) with 5 mM EGTA and protease inhibitor mixture (1836170, complete Mini EDTA Free; Roche Diagnostics GmbH, Germany) and centrifuged at 10,000g for 15 min. Supernatant protein was subjected to electrophoresis, transferred to a PVDF membrane, and probed with either anti-S100A1-Ab (SA 5632, custom made) or anti-cardiac α-actin-Ab (Ac1-20.4.2, Progen). Blots were developed with the Avidix chemiluminescence detection system (Tropix, Applied Biosystems, Foster City, CA, USA), quantified by densitometry, and normalized to actin.

Immunohistochemistry. Immunohistochemistry was performed as described previously [35]. Briefly, cryosections (10 μm) of AdS100A1- and AdGFP-treated LV were permeabilized and incubated with rabbit anti-S100A1-Ab (SA 5632, custom made). Peroxidase-conjugated secondary antibodies and Vector VIP peroxidase substrate kit (Vector Laboratories, Burlingame, CA, USA) was used to reveal the antigen. Rabbit IgG (Santa Cruz Technologies, Santa Cruz, CA, USA) was used as negative control.

RNA isolation and real-time RT-PCR. Total RNA was isolated from left ventricular tissue as well as from isolated cardiomyocytes using either Ultraspec (Biotec) or Trizol (Life Technologies) according to the company's recommendations. cDNA was synthesized by reverse transcription of the RNA with Superscript II (Life Technologies) as recommended. Real-time PCR was performed in duplicate with a 1:100 dilution of the cDNA on a MyIQ real-time PCR detection system (Bio-Rad) with the SYBR Green PCR Master Mix (Applied Biosystems). The oligonucleotide primers to examine expression of genes were as follows: ANF forward primer (FWD) 5′-TGCCGGTAGAAGATGAGGTC-3′, reverse primer (REV) 5′-TGCTTTTC-AAGAGGGCAGAT-3′, NCX FWD 5′-CGAGACTGTGTCGAACCTGA-3′,

REV 5′-TCAGGGACCACGTAAACACA-3′, SERCA2a FWD 5′-TGAGACGCT-CAAGTTTGTGG-3′, REV 5′-ATGCAGAGGGCTGGTAGATG-3′, PLB FWD 5′-TACCTCACTCGCTCGGCTAT-3′, REV 5′-GATGCAGATCAGCAGCA-GAC-3′, S100A1 (rat) FWD 5′-CCATGGAGACC-CTCATCAAT-3′, REV 5′-TGGAAGTCCACTTCCCCATC-3′, S100A1 (total) FWD 5′-CGATGGAGA-CCCTCATCAAC-3′, REV 5′-TGGAAGTCCACCTCCCCGTC-3′, and GRK2 FWD 5′-CCCTCTCACCATCTCTGAGC-3′, REV 5′-CGGTTGGGGAACAAG-TAGAA-3′. For normalization, 18S rRNA was used (FWD 5′-TCAAGAAC-GAAAGTCGGAGG-3′, REV 5′-GGACATCTAAGGGCATCAC-3′). PCR conditions were 95°C for 3 min and 40 cycles of 95°C for 10 s, 63.5°C for 45 s. Specificity of PCR products was confirmed by gel electrophoresis.

Statistical analysis. Data are expressed as means ± SEM. Paired data were evaluated by Student's *t* test. One way ANOVA with Bonferroni's post hoc test or repeated-measures ANOVA was used for multiple comparisons. For all tests, a value of $P < 0.05$ was accepted as statistically significant.

REFERENCES

1. Cohn, J. N. (1997). Report of the National Heart, Lung, and Blood Institute Special Emphasis Panel on Heart Failure Research. *Circulation* **95**(4): 766–770 (Feb 18).
2. American Heart Association (2004). Heart disease and stroke statistics. Online at http://www.americanheart.org.
3. Kato, K., Kimura, S., Haimoto, H., and Suzuki, F. (1986). S100a0 (alpha alpha) protein: distribution in muscle tissues of various animals and purification from human pectoral muscle. *J. Neurochem.* **46**: 1555–1560.
4. Most, P., *et al.* (2001). S100A1: a regulator of myocardial contractility. *Proc. Natl. Acad. Sci. USA* **98**: 13889–13894.
5. Most, P., *et al.* (2003). Transgenic overexpression of the Ca²⁺ binding protein S100A1 in the heart leads to increased in vivo myocardial contractile performance. *J. Biol. Chem.* **278**: 33809–33817.
6. Most, P., *et al.* (2005). Distinct subcellular location of the Ca²⁺ binding protein S100A1 differentially modulates Ca²⁺ cycling in ventricular rat cardiomyocytes. *J. Cell Sci.* **118**: 421–431.
7. Most, P., *et al.* (2003). Extracellular S100A1 protein inhibits apoptosis in ventricular cardiomyocytes via activation of the extracellular signal-regulated protein kinase 1/2 (ERK1/2). *J. Biol. Chem.* **278**: 48404–48412.
8. Remppis, A., *et al.* (1996). Altered expression of the Ca²⁺-binding protein S100A1 in human cardiomyopathy. *Biochim. Biophys. Acta* **1313**: 253–257.
9. Most, P., *et al.* (2004). Cardiac adenoviral S100A1 gene delivery rescues failing myocardium. *J. Clin. Invest.* **114**: 1550–1563.
10. Kettlewell, S., Most, P., Currie, S., Koch, W. J., Smith, G. L. (2005). S100A1 increases the gain of excitation–contraction coupling in isolated rabbit ventricular cardiomyocytes. *J. Mol. Cell. Cardiol.* (in press).
11. Most, P., *et al.* (2003). The C terminus (amino acids 75-94) and the linker region (amino acids 42-54) of the Ca²⁺-binding protein S100A1 differentially enhance sarcoplasmic Ca²⁺ release in murine skinned skeletal muscle fibers. *J. Biol. Chem.* **278**: 26356–26364.
12. Yamasaki, R., *et al.* (2001). Titin–actin interaction in mouse myocardium: passive tension modulation and its regulation by calcium/S100A1. *Biophys. J.* **81**: 2297–2313.
13. Du, X. J., *et al.* (2002). Impaired cardiac contractility response to hemodynamic stress in S100A1-deficient mice. *Mol. Cell. Biol.* **22**: 2821–2829.
14. Emani, S. M., *et al.* (2003). Catheter-based intracoronary myocardial adenoviral gene delivery: importance of intraluminal seal and infusion flow rate. *Mol. Ther.* **8**: 306–313.
15. Hajjar, R. J., *et al.* (1998). Modulation of ventricular function through gene transfer in vivo. *Proc. Natl. Acad. Sci. USA* **28**: 5251–5256.
16. Shah, A. S., *et al.* (2001). In vivo ventricular gene delivery of a beta-adrenergic receptor kinase inhibitor to the failing heart reverses cardiac dysfunction. *Circulation* **6**: 1311–1316.
17. Maurice, J. P., *et al.* (1999). Enhancement of cardiac function after adenoviral-mediated in vivo intracoronary beta2-adrenergic receptor gene delivery. *J. Clin. Invest.* **104**: 21–29.
18. Hata, J. A., Williams, M. L., and Koch, W. J. (2004). Genetic manipulation of myocardial beta-adrenergic receptor activation and desensitization. *J. Mol. Cell. Cardiol.* **37**: 11–21.
19. Rockman, H. A., *et al.* (1991). Segregation of atrial-specific and inducible expression of an atrial natriuretic factor transgene in an in vivo murine model of cardiac hypertrophy. *Proc. Natl. Acad. Sci. USA* **88**: 8277–8281.
20. Chien, K. R., *et al.* (1993). Transcriptional regulation during cardiac growth and development. *Annu. Rev. Physiol.* **55**: 77–95.
21. Remppis, A., *et al.* (2002). The small EF-hand Ca²⁺ binding protein S100A1 increases contractility and Ca²⁺ cycling in rat cardiac myocytes. *Basic Res. Cardiol.* **97**: I56–I62.
22. Remppis, A., *et al.* (2004). S100A1 gene transfer: a strategy to strengthen engineered cardiac grafts. *J. Gene Med.* **6**: 387–394.
23. Anand, I. S. (2000). Ventricular remodeling without cellular contractile dysfunction. *J. Card. Fail.* **8**: S401–S408.
24. Gosselin, H., Qi, X., and Rouleau, J. L. (1998). Correlation between cardiac remodeling, function, and myocardial contractility in rat hearts 5 weeks after myocardial infarction. *Can. J. Physiol. Pharmacol.* **76**: 53–62.
25. Gaballa, M. A., and Goldman, S. (2002). Ventricular remodeling in heart failure. *J. Card. Fail.* **8**(6 Suppl.): S476–S485.
26. Rabinowitz, J. E., *et al.* (2002). Cross-packaging of a single adeno-associated virus (AAV) type 2 vector genome into multiple AAV serotypes enables transduction with broad specificity. *J. Virol.* **76**: 791–801.
27. Ciulla, M. M., *et al.* (2004). Left ventricular remodeling after experimental myocardial cryoinjury in rats. *J. Surg. Res.* **116**: 91–97.
28. Zimmermann, W. H., *et al.* (2002). Cardiac grafting of engineered heart tissue in syngenic rats. *Circulation* **106**: I151–I157.
29. Haider, H. K. H., Tan, A. C., Aziz, S., Chachques, J. C., and Sim, E. K. (2004). Myoblast transplantation for cardiac repair: a clinical perspective. *Mol. Ther.* **9**: 14–23.
30. Tsoporis, J. N., Marks, A., Zimmer, D. B., McMahon, C., and Parker, T. G. (2003). The myocardial protein S100A1 plays a role in the maintenance of normal gene expression in the adult heart. *Mol. Cell. Biochem.* **242**: 27–33.
31. Engelhard, S., Hein, L., Wiesmann, F., and Lohse, M. J. (1999). Progressive hypertrophy and heart failure in beta1-adrenergic receptor transgenic mice. *Proc. Natl. Acad. Sci. USA* **96**: 7059–7064.
32. He, T. C., Zhou, S., da Costa, L. T., Yu, J., Kinzler, K. W., and Vogelstein, B. (1998). A simplified system for generating recombinant adenoviruses. *Proc. Natl. Acad. Sci. USA* **95**: 2509–2514.
33. Huwer, H., Winning, J., Vollmar, B., Welter, C., Menger, M. D., and Schafers, H. J. (2000). Model of chronic systolic and diastolic dysfunction after cryothermia-induced myocardial necrosis in rats. *Comp. Med.* **50**: 385–390.
34. Cho, M. C., Rapacciuolo, A., Koch, W. J., Kobayashi, Y., Jones, L. R., and Rockman, H. A. (1999). Defective beta-adrenergic receptor signaling precedes the development of dilated cardiomyopathy in transgenic mice with calsequestrin overexpression. *J. Biol. Chem.* **274**(32): 22251–22256 (Aug 6).
35. Zhou, R. H., Yao, M., Lee, T. S., Zhu, Y., Martins-Green, M., and Shyy, J. Y. (2004). Vascular endothelial growth factor activation of sterol regulatory element binding protein: a potential role in angiogenesis. *Circ. Res.* **95**: 471–478.